



HAL
open science

Vertically aligned carbon nanotubes on aluminum foils from biosourced precursors: Application to energy storage

Corentin Chatelet, Ugo Forestier-Colleoni, Philippe Banet, Jérémie Descarpentries, Thomas Goislard de Monsabert, Fabien Nassoy, Cécile Reynaud, Mathieu Pinault

► To cite this version:

Corentin Chatelet, Ugo Forestier-Colleoni, Philippe Banet, Jérémie Descarpentries, Thomas Goislard de Monsabert, et al.. Vertically aligned carbon nanotubes on aluminum foils from biosourced precursors: Application to energy storage. Carbon Trends, 2025, 19, pp.100450. 10.1016/j.cartre.2024.100450 . hal-04926424

HAL Id: hal-04926424

<https://hal.science/hal-04926424v1>

Submitted on 3 Feb 2025

HAL is a multi-disciplinary open access archive for the deposit and dissemination of scientific research documents, whether they are published or not. The documents may come from teaching and research institutions in France or abroad, or from public or private research centers.





L'archive ouverte pluridisciplinaire **HAL**, est destinée au dépôt et à la diffusion de documents scientifiques de niveau recherche, publiés ou non, émanant des établissements d'enseignement et de recherche français ou étrangers, des laboratoires publics ou privés.



Distributed under a Creative Commons Attribution - NonCommercial - NoDerivatives 4.0 International License



Vertically aligned carbon nanotubes on aluminum foils from biosourced precursors: Application to energy storage

Corentin Chatelet^{a,b,c} , Ugo Forestier-Colleoni^a, Philippe Banet^c , Jérémie Descarpentries^b, Thomas Goislard de Monsabert^b, Fabien Nassouy^{a,b}, Cécile Reynaud^a , Mathieu Pinault^{a,*} 

^a Université Paris-Saclay, CEA, CNRS, NIMBE 91191, Gif-sur-Yvette, France

^b NAWAH, 250 Av. Villevieille, 13790 Rousset, France

^c CY Cergy Paris Université, LPPI F-95000, Cergy, France

ARTICLE INFO

Keywords:

Vertically aligned carbon nanotubes
Aerosol-assisted catalytic chemical vapour deposition
Biobased precursors
Energy storage, Energy of activation

ABSTRACT

Vertically aligned carbon nanotubes (VACNTs) are among the nanomaterials recognized as efficient for many applications, such as thermal management or energy storage. Since they are mainly produced from hydrocarbon precursors, one of the issue is to reduce the carbon footprint of their synthesis by using bio-sourced precursors. Herein, we use bio-based carbon precursors to effectively grow VACNTs on aluminum thin foils from a one-step catalytic chemical vapor deposition (CCVD) method. This process at moderate temperature and atmospheric pressure is cost-effective and produces good-quality VACNTs on a large scale. We show that we can replace C₂H₂ with bio-sourced carbon precursors, and also toluene, which acts as a solvent for ferrocene, with more eco-friendly solvents. We observe that the activation energy of the growth process depends significantly on the precursor. After a selection of compatible carbon precursors and a parametric study, a 100 μm high VACNT carpet was obtained on Al foils with ethylene and butanol as carbon precursors and ferrocene solvent respectively. The VACNT samples were directly tested as supercapacitor electrodes. The results show that the volumetric capacitances obtained with bio-based precursors match those obtained with acetylene as the carbon precursor.

1. Introduction

To limit the effects of global warming, industry must take a huge leap to become carbon free, as it is responsible for 23 % of CO₂ emissions at global scale [1]. This statement must also apply to the production of nanomaterials, which are considered essential for applications in favor of environmental sustainability [2]. In particular, vertically aligned carbon nanotubes (VACNTs) are good candidates for a lot of such applications [3], including electrodes for energy storage systems [4,5]. As VACNTs are mainly produced by catalytic chemical vapor deposition (CCVD) from hydrocarbon precursors [6], our aim is to replace those derived from fossil resources with precursors derived from biomass. Using biomass closes the carbon cycle as the CO₂ used by the plant to grow offsets that released into the air [7].

The production of carbon nanotubes from biomass is developing, mainly for their production in bulk by pyrolysis of natural products [8]. Regarding the production of VACNTs by CCVD, early research in the literature focused on the use of natural oils [9–13] or camphor [14] as

carbon precursors. Most of the studies were carried out at temperature above 750 °C, and with camphor, the maximum VACNT height is 2 mm after 1.5 h of synthesis at 850 °C [15]. However, these compounds of high molecular weight are not reactive enough to be efficient at lower temperature. Indeed, only one study reports VACNT growth under 700 °C with them and VACNT height is just a few μm [16].

The issue is that for many applications, such as growth on aluminum foil, the CCVD temperature needs to be much lower. This is why acetylene is the most widely used carbon precursor for VACNT growth at low temperature due to its high reactivity [17]. Unfortunately, acetylene is prepared by hydrolysis of CaC₂, a process generating 2.24 kgCO₂eq. kg-prod⁻¹ due to the use of coal [18]. The challenge is therefore to find biosourced precursors with sufficient reactivity to be viable in the CCVD process and whose production is less carbon-intensive.

We propose to take advantage of the rapid development of the bio-refinery, the transformation of vegetal products like cereals by fermentation into alcohols or gases [19], to find suitable precursors with lower molecular weight. We focus first on molecules that have shown

* Corresponding author.

E-mail address: mathieu.pinault@cea.fr (M. Pinault).

<https://doi.org/10.1016/j.cartre.2024.100450>

Received 6 September 2024; Received in revised form 20 December 2024; Accepted 20 December 2024

Available online 21 December 2024

2667-0569/© 2024 The Authors. Published by Elsevier Ltd. This is an open access article under the CC BY license (<http://creativecommons.org/licenses/by/4.0/>).

promising VACNT growth at low temperatures. It is the case of ethanol, which is the main product of biorefinery. With standard ethanol, heights of 90 μm [20] and 60 μm [21] were obtained in 30 min at temperatures below 660 °C on Al. Another candidate could be ethylene, the bio-based version of which comes from the catalytic dehydration of ethanol. It has been widely used, in its standard form, as a carbon source for VACNT synthesis, but on Al, few studies exist that report growths of 80 μm in 40 min at 640 °C [22] or 22 μm in 15 min under similar conditions [23]. The most innovative part of our approach is to try out other molecules whose standard form has not yet been used in CCVD but whose bio-sourced production is being actively developed because they are in demand as biofuels or biochemical [24]. This is the case for molecules with 4 carbon atoms, such as butanol, isobutene and ethyl acetate. All these precursors are compared for VACNT synthesis but also their mixture, as studies report beneficial synergistic effects when using a mixture of precursors [25,26].

The aerosol-assisted CCVD was selected since this simple one-step process leads to the rapid and continuous growth of dense VACNTs [27–29] and is well adapted to the industrial scale [30–32]. In one-step CCVD, carbon and metal precursors are injected simultaneously, so that the catalytic particles are formed in-situ and refreshed continuously during synthesis, thus limiting their poisoning. With this process, high VACNT thickness and growth rate are easily reached at high temperature (>750 °C) on silicon, quartz and other substrates [27] with ferrocene as catalyst precursor. At low temperature (<660 °C) on commercial aluminum foil, a significant growth rate was obtained using acetylene as the carbon precursor [29,30,33,34].

In the present paper, we will replace C_2H_2 by the bio-sourced carbon precursors discussed above, adding camphor for comparison (Table 1). These precursors differ in their molecular weight, but also in their C/O ratio, as all the selected liquid precursors contain oxygen. These liquids can be used as a solvent for ferrocene, thus advantageously replacing toluene with an eco-friendly solvent. For the most promising precursors or mixtures of precursors, a parametric study is performed where H_2 content, synthesis temperature and duration are evaluated. It is then shown that a 100 μm high carpet of VACNTs can be obtained on Al foils with an original mixture of ethylene and butanol as carbon precursor. The activation energy of the process is determined and discussed as a function of the precursor. Structural and electrochemical characterizations of the samples are performed to evaluate their interest as electrode for energy storage applications. Finally, the up scaling of the process is reported with its best performances.

2. Method

VACNT are synthesized on aluminum substrates through the aerosol-assisted CCVD process, operated at atmospheric pressure in a set-up adapted from those described previously [27,34,41,42]. The chemicals used through this study are not bio-based but are and will be commercially accessible in their bio-based version. The catalytic precursor (ferrocene, 99 %, Acros Organics) is dissolved in toluene (99.9 %, Merck) or in one of the different bio-sourced carbon liquid precursors:

ethanol (anhydrous, Carlo Erba Reagent S.A.S), butanol (99.9 %, Analytical grade), ethyl acetate (99.8 %, anhydrous, Merck), camphor oil (Camphor white oil, Kosher, Sigma-Aldrich).

The mix is injected as an aerosol through an engine injection system (Qualiflow-Jipelec) and carried by a gas flow of Ar and H_2 into a reactor placed in a furnace set at a temperature well below the Al melting point (660 °C) [29]. Two new gases are tested to grow VACNTs: ethylene (N35, Air Liquide) and isobutene (Air Liquide), while acetylene (Messer) is used as reference. Total flow of all gases is set at 100 sccm while ethylene, isobutene and acetylene flow are set at 15 sccm. Argon flow is adjusted to reach the 100 sccm flow.

Ten thin Al discs of 1.2 cm in diameter from Korff foils (40 μm thick, purity 99.5 % with Si as main impurity) are placed in the isothermal area of the reactor at 17 to 28 cm from the furnace entrance. No specific pre-treatment of the Al surface (except acetone cleaning) is required. Two synthesis temperatures are tested: 615 °C and 640 °C. The samples are weighed before and after the synthesis.

The thickness and morphology of the VACNT carpets obtained on the first and last Al discs are observed by Scanning Electron Microscopy (SEM, Carl Zeiss Ultra 55). The thicknesses reported in the following results are an average of three measurements taken on the cross-sections of the first and last samples, which are representative of all the VACNT samples along the reactor.

CNT structure and diameter are determined by Transmission Electron Microscopy (TEM, Philips CM 12, 120 kV) after ultrasonic dispersion of CNTs in pure ethanol and deposit on lacey carbon film on copper grids. The mean inner and outer diameters are obtained from the observation of at least 100 CNTs per sample. Raman analyses (Renishaw Invia Reflex, $\lambda_{\text{laser}} = 532 \text{ nm}$, $P_{\text{laser}} = 2 \text{ mW}$) are performed from top view of the carpets.

Energy of activation is calculated from Arrhenius' law using VACNT growth rate taken at 20 min at three different temperature. VACNT heights obtained at 20 min synthesis duration are used because under our growth conditions the height increased almost linearly with duration up to 20 min and even beyond (see Supplementary data). Additionally, growth rate ($\mu\text{m}\cdot\text{min}^{-1}$) is taken instead of mass rate ($\text{mg}\cdot\text{min}^{-1}$) because density does not increase with increasing temperature (see Supplementary Data).

Electrochemical characterizations are performed with a multi-channel potentiostat/galvanostat (VSP-150, Biologic Scientific Instrument). A three-electrode cell configuration is used with VACNT/Al as working electrode, Ag wire as reference electrode and porous carbon as counter electrode [29]. The electrolyte is a mixture of 1-ethyl-3-methylimidazolium bis(trifluoromethanesulfonyl)imide (EMITFSI, 99 %, Solvionic) and acetonitrile (ACN, 99.5 %, VWR International), both used as received. The molar concentration is 1.3 M of EMITFSI in ACN. Cyclic voltammetry measurements are performed at different scan rates (5, 10, 20, 50, 100, 200 and 500 mV/s) between -0.3 and 1.0 V . The capacitance (C in F), the volumetric capacitance (C_v in $\text{F}\cdot\text{cm}^{-3}$), as well as the developed surface area of VACNTs on the Al disc (S_{dev} in m^2) are determined from raw electrochemical data and from VACNT geometric data.

3. Results and discussion

3.1. VACNT synthesis at 615 °C on aluminum

Six different bio-sourced carbon precursors are tested for VACNT synthesis: ethanol, butanol, ethyl acetate, camphor oil, ethylene and isobutene. Ferrocene is directly dissolved in the four liquid carbon sources. The ferrocene concentration was set at 2 w% for butanol and ethanol which is the maximum that can be dissolved in these liquids, while for ethyl acetate, it was optimized and set at 5 w%. Finally, for ethylene and isobutene, ferrocene is dissolved in toluene with a concentration of 2.5 w%, value optimized from previous work [29].

Table 1

Thermodynamic and chemical properties of the precursors assessed in this study.

Precursor	Formula	Molar mass (g/mol)	O/C ratio	Evaporation temperature (°C)	Standard enthalpy of formation (kJ.mol ⁻¹)
Ethylene	C_2H_4	28	0	-103.9	52 [35]
Isobutene	$\text{H}_2\text{C}=\text{C}(\text{CH}_3)_2$	56	0	-6.93	-134 [36]
Camphor	$\text{C}_{10}\text{H}_{16}\text{O}$	152	1/10	179.75	-319 [37]
Butanol	$\text{C}_4\text{H}_{10}\text{O}$	74	1/4	117	-328 [38]
Ethanol	$\text{C}_2\text{H}_6\text{O}$	46	1/2	79	-277 [39]
Ethyl acetate	$\text{C}_4\text{H}_8\text{O}_2$	88	1/2	77.1	-480 [40]

Synthesis duration is set at twenty minutes and the oven temperature at 615 °C. The H₂ content in the gas flow is adjusted to 10 vol%. These conditions were determined to be optimal for VACNT growth with acetylene in our set-up [29,33,34].

As shown by SEM observations (Fig. 1), a VACNT carpet is obtained under these conditions on Al collectors regardless of the carbon precursor selected. The carpets measure between 7 and 12 μm. This shows that each selected chemical can decompose into VACNT precursors at 615 °C with 10 % H₂. However, the short heights obtained show that, as expected, the chemicals are less reactive than acetylene, which leads to a height of about 100 μm in 20 min [29,34].

Camphor oil and isobutene were eliminated from the study as they doesn't respond to the criteria previously mentioned. Camphor oil was hard to use with our injector system due to the high viscosity. Bio-based version of isobutene is not commercially available at high volume. Only ethanol-derived products were kept.

The previous conditions optimized for acetylene give lower VACNT growth rate with these new precursors. To improve the rate, we will first study the impact of the H₂ content in the gas phase, as this is an important parameter in catalytic CVD. Firstly, it has an impact on the ferrocene decomposition rate and therefore on the formation of catalytic particles [42]. Secondly, it affects the chemical species present in the reactor [43] and prevents the pyrolytic carbon formation. Finally, H₂ can also act as an etchant to remove carbon byproducts, such favoring the activity of catalyst particles [44]. New syntheses were performed with increased H₂ content to 30 vol% and 50 vol% (Table 2). VACNT growth without H₂ was also evaluated.

As can be seen from Table 2, no growth occurs at 0 vol% H₂. This can be explained by the crucial effect of H₂ on the dissociation of ferrocene, which becomes possible well below 800 °C, allowing the formation of catalytic particles [42]. In the presence of H₂, its content has a different impact depending on the precursor. On the one hand, hydrogen seems to have little impact when ethanol and butanol are used, as no major change in VACNT height is observed. On the other hand, in the case of ethylene, the VACNT height increases from 7 μm to 21 μm when increasing the H₂ content to 50 vol% and for ethyl acetate from 8 μm to 16 μm when increasing the hydrogen content to 30 vol%.

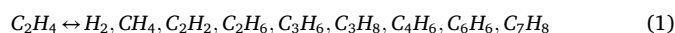
To explain the large difference between ethylene and the other precursors, an etching effect does not seem sufficient, as it would affect all cases. On the other hand, the competition between hydrogenation

Table 2

Influence of H₂ content in the gas flow and reactor temperature on the mean value and standard deviation of VACNT height after 20 min synthesis duration.

Temperature (°C)	Hydrogen content (vol.%)	Ethylene (ferrocene dissolved in toluene)	Ethanol	Butanol	Ethyl acetate
615	0 %	No growth			
	10 %	7 ± 1 μm	11 ± 2 μm	13 ± 1 μm	8 ± 2 μm
	30 %	14 ± 4 μm	12 ± 1 μm	12 ± 1 μm	15.8 ± 0.1 μm
640	50 %	21 ± 3 μm	11 ± 1 μm	9 ± 1 μm	12 ± 3 μm
			20 ± 7 μm	19 ± 7 μm	20 ± 10 μm

and thermal decomposition seems better able to interpret this result. Indeed the thermal decomposition of ethylene is complex because it produces a lot of hydrocarbon as well as H₂ [26,45] (Equation (1)(Eq. (2)):



Based on Le Châtelier principle, the addition of H₂ could slow down the ethylene thermal decomposition (Eq. (1)) and shift the gas phase composition to a more favorable one for VACNT growth. For the others precursors, the addition of H₂ doesn't affect gas phase chemistry as the main thermal decomposition products is water [46–48] and hydrogenation cannot occur. For the following syntheses H₂ content in gas flow is kept at 50vol%.

3.2. VACNT synthesis at 640 °C on aluminum

As demonstrated above, at 615 °C, VACNT carpets were obtained for each precursor but with a low growth rate due to low reactivity. As VACNT synthesis is a thermo-activated catalytic reaction, increasing the temperature is a powerful tool to improve the VACNT growth. Therefore, we set the following synthesis temperature at 640 °C with 50 vol% H₂ for each precursor, as in addition; the aluminum substrate already

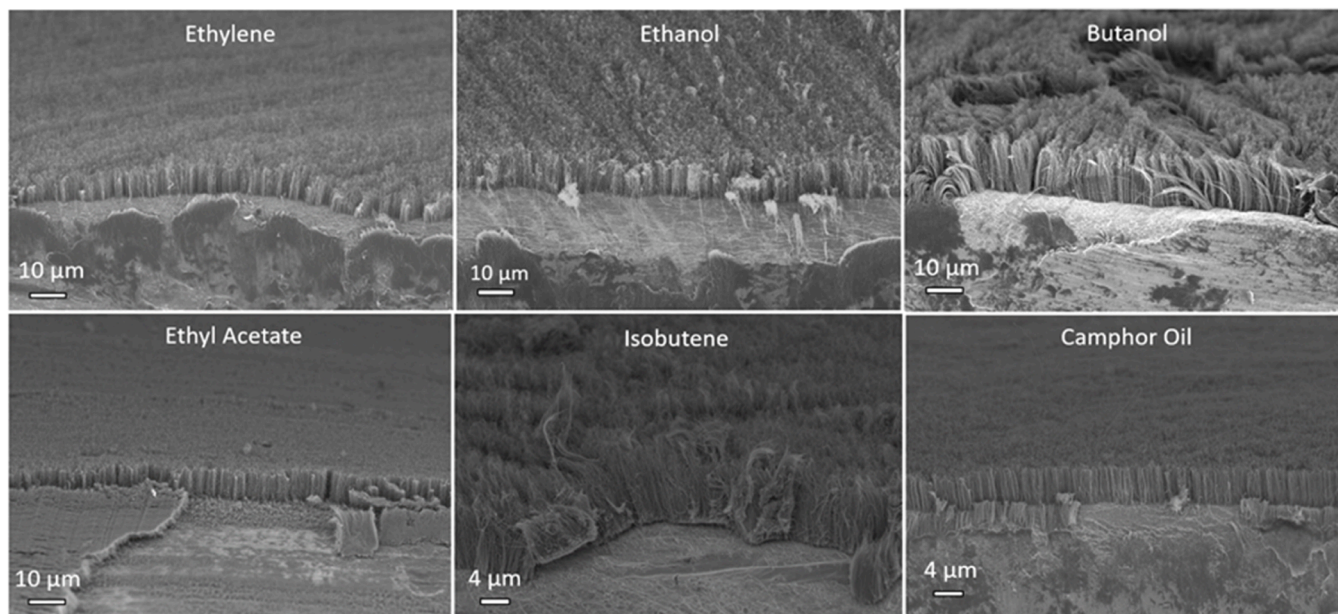


Fig. 1. SEM pictures of VACNT carpets synthesized at 615 °C with 10 % H₂.

showed resistance to these conditions.

As expected, increasing the synthesis temperature by 25 °C drastically improves VACNT growth as the mean carpet height increases for all precursors (Table 2). With ethylene, it increases from 21 μm to 24 μm in mean value when the others nearly double their VACNT height: from 11 μm to 20 μm for ethanol, from 9 μm to 19 μm for butanol and from 12 μm to 20 μm for ethyl acetate. As the temperature increases, the dispersion in height is larger at 640 °C than at 615 °C. We can also see the appearance of overgrown material on the top of the carpet for ethylene, phenomenon previously reported in literature [49] (Fig. 2).

For ethanol, butanol and ethyl acetate, the VACNT height on the first Al disc in the reactor is higher than the one on the last disc upon the temperature increase, probably due to the fact that more precursors are consumed earlier in the reactor during the process at 640 °C. However for (ethylene + toluene), the carpet is higher for the last Al disc than on the first disc. This opposite behavior is yet to be understood. For the areal mass, all the precursors give homogenous results alongside the reactor with a slight decrease in areal mass from the first to the last sample (Fig. 3).

The temperature increase seems to have a greater impact in the case of ethanol, butanol and ethyl acetate than in the case of ethylene, as the VACNT height is almost doubled. This can be explained by a difference in activation energy, the minimum energy required to initiate the growth of VACNT. Its value is that of the limiting step in the growth process [6]. Additional syntheses at 630 °C were done with ethylene, butanol, ethanol, and ethyl acetate and at 615 °C, 630 °C and 640 °C with acetylene to complete the study.

As deduced from the data plotted in Fig. 4 the precursors have very different activation energies. Ethylene, ethyl acetate and acetylene have an activation energy below 1.5 eV which means that the synthesis is driven by bulk diffusion into the catalyst, while synthesis with ethanol and butanol, with activation energy of 1.9 and 2.7 eV respectively, seems to be driven by precursor decomposition [6,50].

For acetylene, a value of 1.0 eV is found which is lower than that reported in literature [51,52]. However, bulk diffusion was also

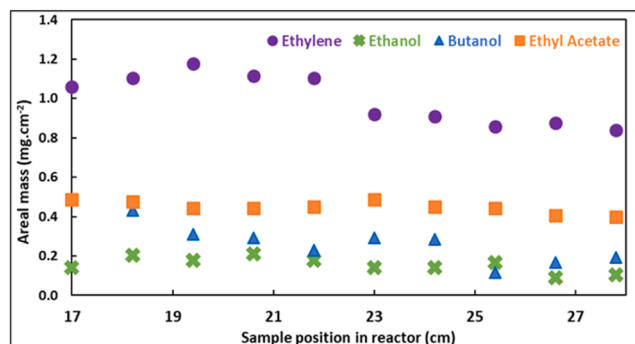


Fig. 3. Areal mass following sample position and precursor.

considered as the limiting step. In addition, as suggested by the literature [25,50], acetylene seems to be the direct precursors of CNTs (Eq. (3)) confirming why synthesis with acetylene are limited by bulk diffusion [53]. σ represent the catalyst particle.



For ethylene, a similar energy of activation was also found by Chen et al. [54] with a sufficient carbon supply. The activation energy value obtained with ethylene in our work indicates that either the ethylene is a direct precursor for CNT growth or the energy required to transform it into acetylene is lower than 1.5 eV (Eq. (4)).



For ethyl acetate, this low value can be attributed to its low temperature of decomposition into ethylene around 600 °C [47].

In the case of butanol and ethanol, whose activation energy is greater than 1.7 eV, the determining step is rather the decomposition of the precursor on the catalytic particle (σ). The literature [25,50] suggests the following dehydration reaction: (Eq. (5)), (Eq. (6)).

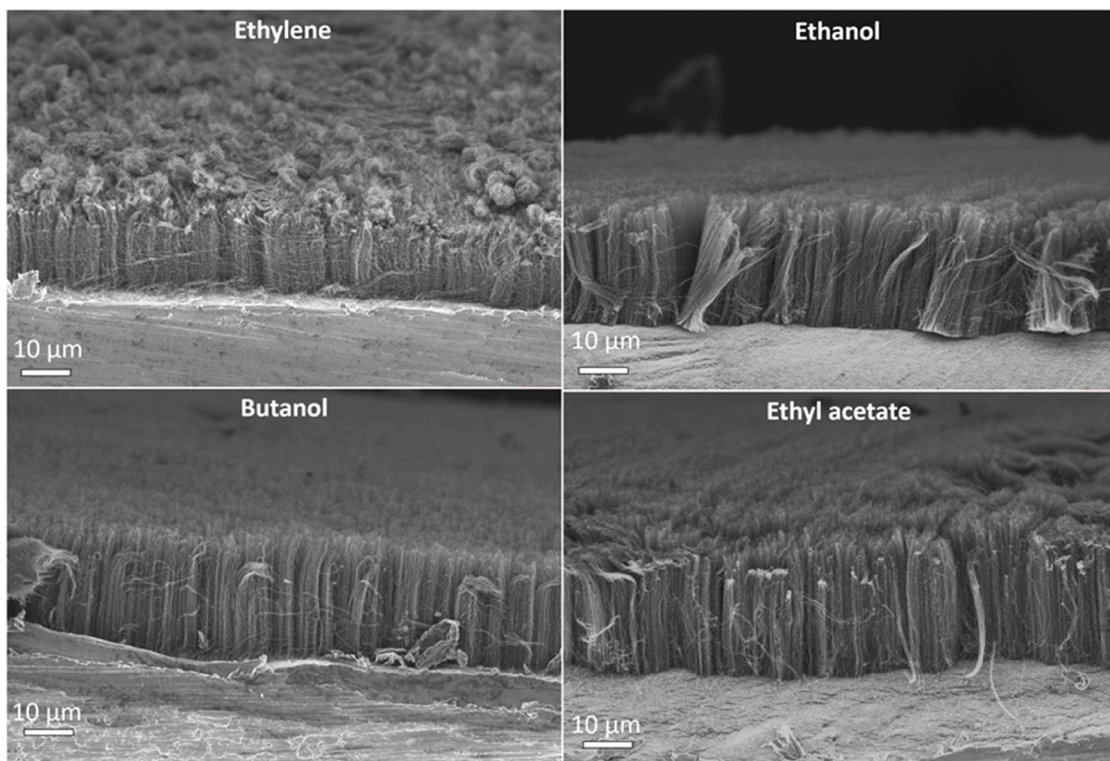


Fig. 2. VACNT carpets synthesized with each of the selected precursors at 640 °C after 20 min synthesis duration.

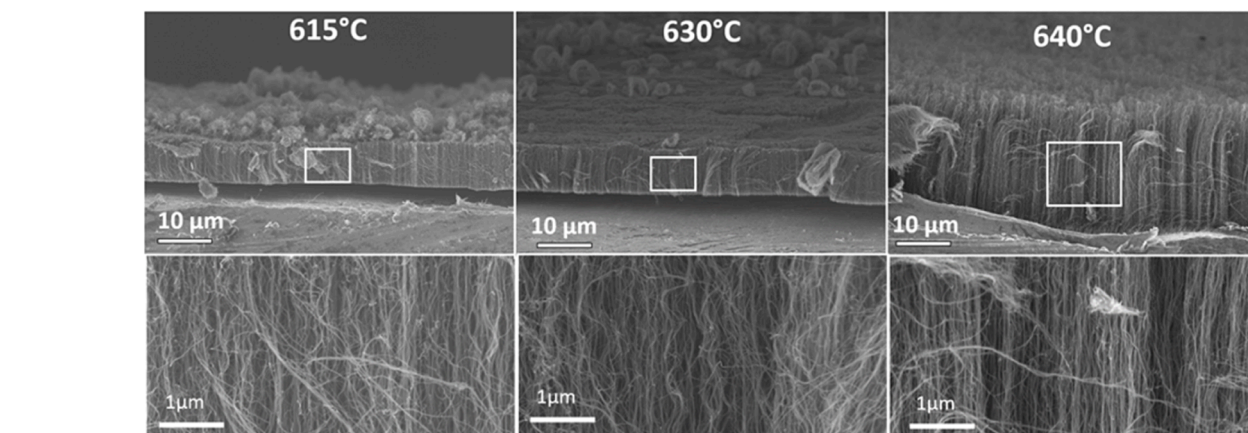
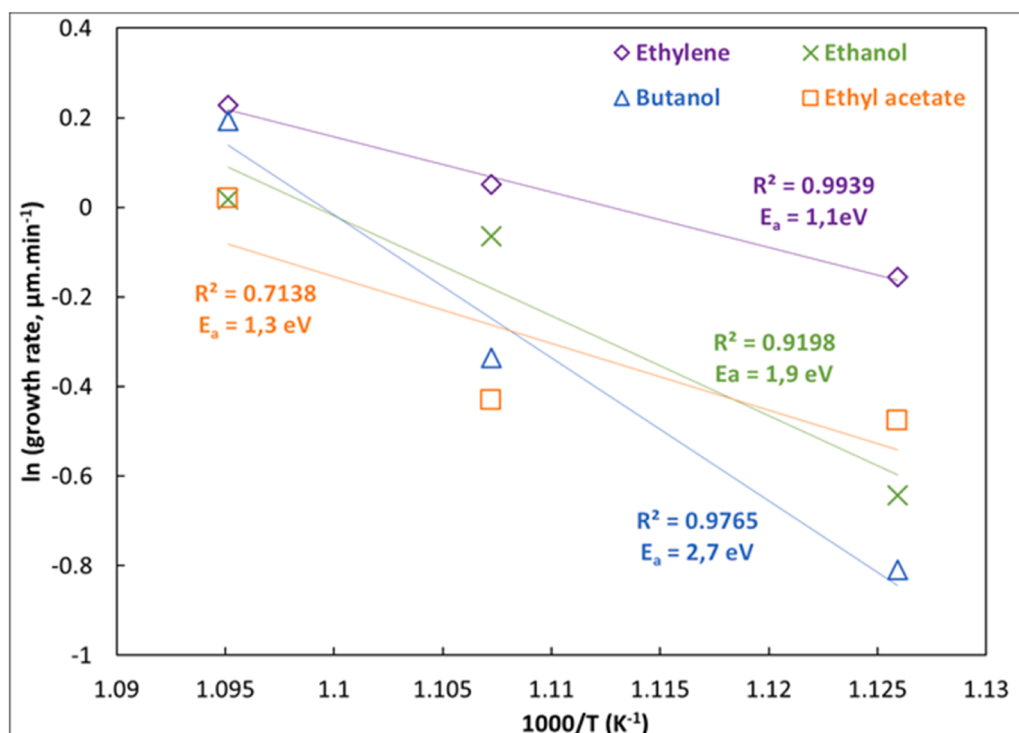
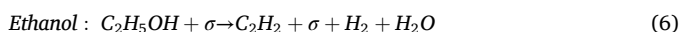
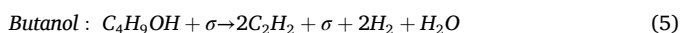


Fig. 4. Top: Growth rate ($\mu\text{m}/\text{min}$) for Ethylene (purple point), Butanol (blue triangle), Ethanol (green cross), Ethyl acetate (orange square) and Acetylene (red star) at three different temperatures: 615 °C, 630 °C, 640 °C as a function of $1000/T$. Activation energy deduced from the fit is indicated in the inserts. Bottom: SEM images of VACNT obtained from Butanol at different synthesis temperatures.



The water produced during the process is likely to oxidize the catalyst particle [55].

3.3. Replacing toluene and the effect of mixing precursors

As stated previously, toluene is the solvent used to dissolve ferrocene in the case of synthesis with ethylene. However, at this temperature, toluene is not reactive [29,34] and doesn't act like a second carbon source. In addition, toluene is classified as health hazard. Thus replacing it by bio-sourced precursors is a solution to have a safer VACNT synthesis process and an addition of carbon input.

Therefore, syntheses were done with ethylene with one of the selected liquids (ethanol, butanol or ethyl acetate) to dissolve ferrocene. At the same time, we are studying the effect of a mixture of two carbon

precursors. The following syntheses were performed at 640 °C with 50 vol% H_2 in the gas flow.

Figs. 5 and 6 show that replacing toluene with the various tested liquids in the synthesis with ethylene induces an increase in VACNT mean height in all cases when compared with the syntheses performed with each of the liquids alone. In addition, the mixture of ethylene with ethanol and ethyl acetate homogenizes the VACNT heights along the reactor as the standard deviations decrease. The addition of ethylene to butanol exhibits a particularly interesting behavior as the VACNT height increases drastically from a mean value of 20 μm to 40 μm which outperforms the values obtained for the VACNT synthesis with (ethylene and toluene). In terms of cleanliness VACNT carpets obtained with ethylene and oxygen-bearing precursors presents less bundles on the surface than the ones with (ethylene + toluene) (Fig. 5) probably because of the etching effect of H_2O formed during their pyrolysis.

Literature reports that mixing carbon sources could increase the VACNT growth rate and yield because of a synergistic effect [25,26]. For example, Shibuya et al. [25] mixed acetylene and 1,3-butadiene at a

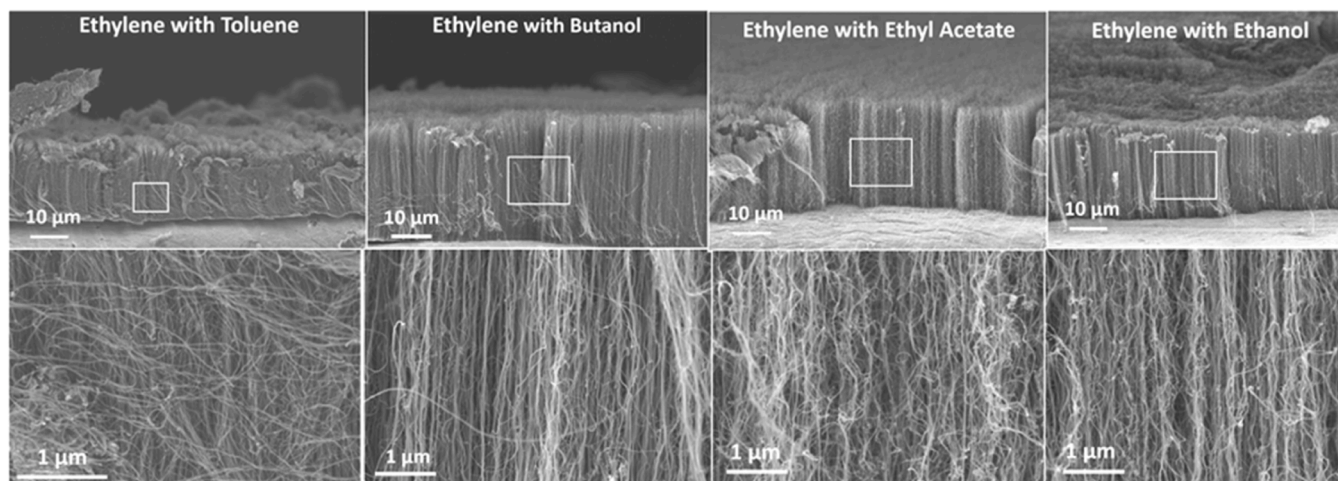


Fig. 5. SEM images of VACNT grown with Ethylene and each liquid precursor after 20 min synthesis duration at 640 °C.

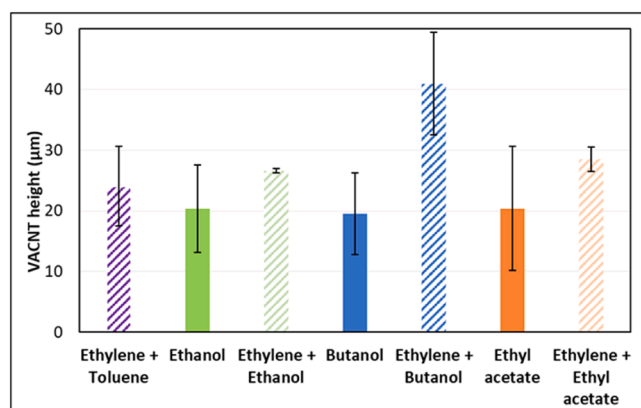


Fig. 6. Impact of replacing Toluene by the tested liquids on VACNT mean height after 20 min synthesis duration at 640 °C with 50 vol% H₂.

ratio of 2:5 at 800 °C obtaining 5 mg.cm⁻² at 0.27 mole of carbon input instead of 2.6 mg.cm⁻² for pure 1,3-butadiene and nearly 0 for pure acetylene due to catalyst poisoning.

In Fig. 7, the VACNT growth rate is plotted as a function of the injected carbon mole rate. Two syntheses with (ethylene + toluene) at higher and lower flow are added to complete the study. We can see that

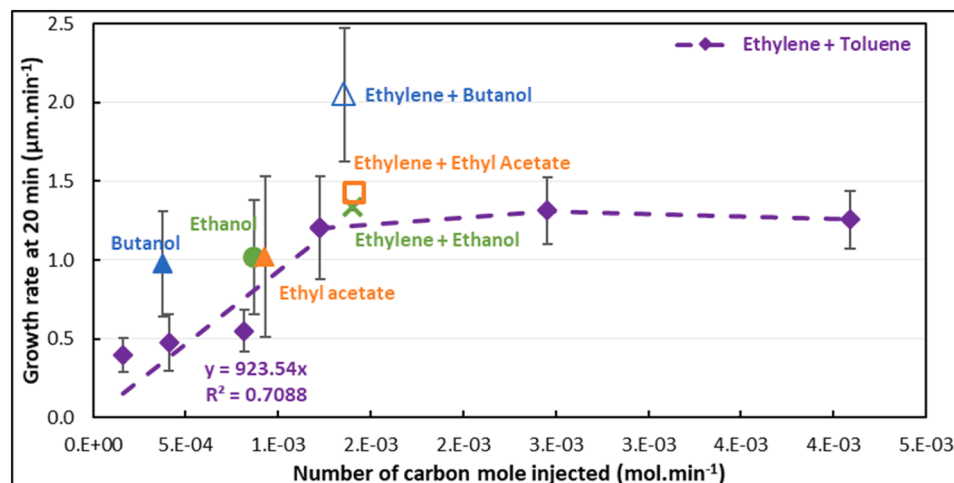


Fig. 7. VACNT apparent growth rate after 20 min synthesis duration as a function of the carbon concentration in the feedstock.

increasing the carbon intake up to $1.2 \cdot 10^{-3} \text{ mol} \cdot \text{min}^{-1}$ increases the growth rate from $0.4 \text{ } \mu\text{m} \cdot \text{min}^{-1}$ to $1.2 \text{ } \mu\text{m} \cdot \text{min}^{-1}$. A plateau seems to be reached after this value. However, the result obtained with (ethylene + butanol) doesn't fit the plot with a higher growth rate per carbon mole compared to other couples like (ethylene + ethanol) and (ethylene + ethyl acetate). This means that a synergistic effect could occur between butanol and ethylene when they are associated in the gas phase.

These results demonstrate that the addition of ethylene to the tested liquids leads to the efficient growth of VACNT on aluminum at low temperature with only bio-based and nonpoisonous precursors.

Turning now to the activation energy for the (ethylene + butanol) and (ethylene + ethanol) pairs (Fig. 8A), its value remains above 1.7 eV as was the case without C₂H₄, indicating that growth is still limited by the decomposition step. For (ethylene + ethyl acetate), the new value of 1.8 eV compared with 1.3 eV without ethylene should be taken with caution as the linear fit is limited with an R² value of only 0.83.

As the ethylene and butanol do not behave in the same way according to the hydrogen percentage in the gas flow, a study of the influence of this parameter on VACNT growth was carried out. As observed in Fig. 8B, the (ethylene + butanol) couple exhibits the same trend as ethylene with toluene: increasing hydrogen in the gas phase increases the VACNT height. Indeed the mean height jumps from $23 \pm 1 \text{ } \mu\text{m}$ for 10 % H₂ to $41 \pm 8 \text{ } \mu\text{m}$ for 50 % H₂.

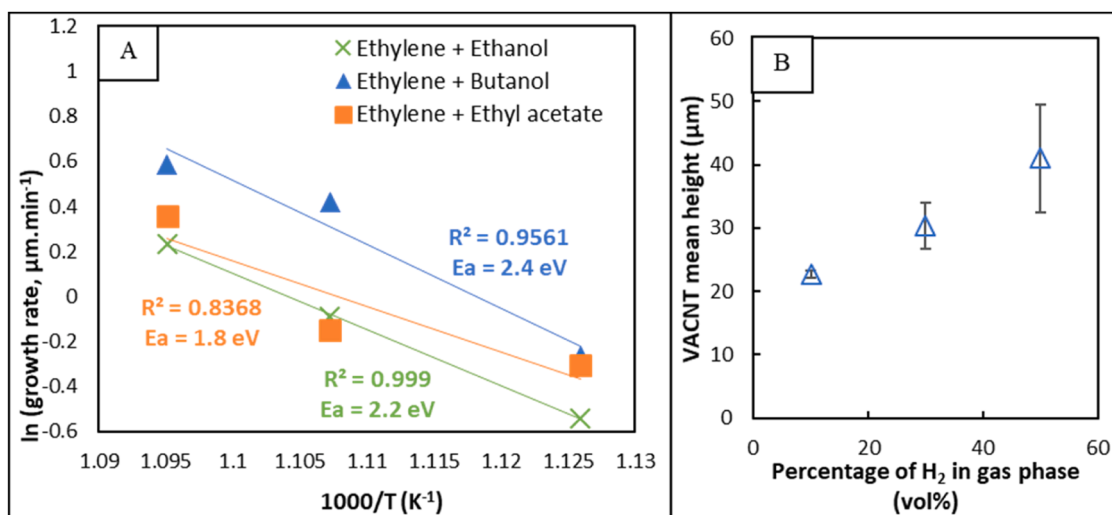


Fig. 8. (A) Energy of activation for Ethylene + Butanol (green cross), Ethylene + Ethyl acetate (orange square) and Ethylene + Ethanol (blue triangle) (B) Influence of the H₂ content on VACNT height with Ethylene + Butanol as precursors.

3.4. Effect of the synthesis duration

In order to increase the final height of the VACNTs, previous synthesis durations were extended to 40 min and 80 min (Figs. 9 and 10). This also allows to check whether some saturation occurs as a result of catalytic deactivation, as often observed at low temperatures [29,34].

On Fig. 9, all VACNT carpets keep growing up to a synthesis duration of 80 min. After 80 min, mean VACNT height from (ethylene + toluene) reaches 99 μm, while it is 89 μm for (ethylene + butanol), 62 μm for (ethylene + ethanol) and 54 μm for (ethylene + ethyl acetate). However, a slight growth rate reduction is present for all precursors except for (ethylene + toluene) where VACNT growth rate is linear with the duration.

Numerous studies have attempted to explain this limitation in thickness as the synthesis duration increases. Authors frequently attribute this decrease in growth rate to either limited feedstock diffusion through the carpet [46,56] or deactivation of catalytic particles [9,14,57] resulting in the complete disruption of VACNT growth [9,14,57,58]. Our previous findings derived from synthesis with acetylene [29,34] were effectively modeled using an exponential decay model (Eq. (7)) that characterizes the self-deactivation of catalytic particles [57,59]. In this model, the parameter "τ" represents the catalyst lifetime, and "h_{max}" the theoretical maximum carpet thickness, calculated as the product of τ and the initial growth rate γ₀.

$$h(t) = \gamma_0 \tau \left(1 - e^{-\frac{t}{\tau}}\right) = h_{\max} \left(1 - e^{-\frac{t}{\tau}}\right) \quad (7)$$

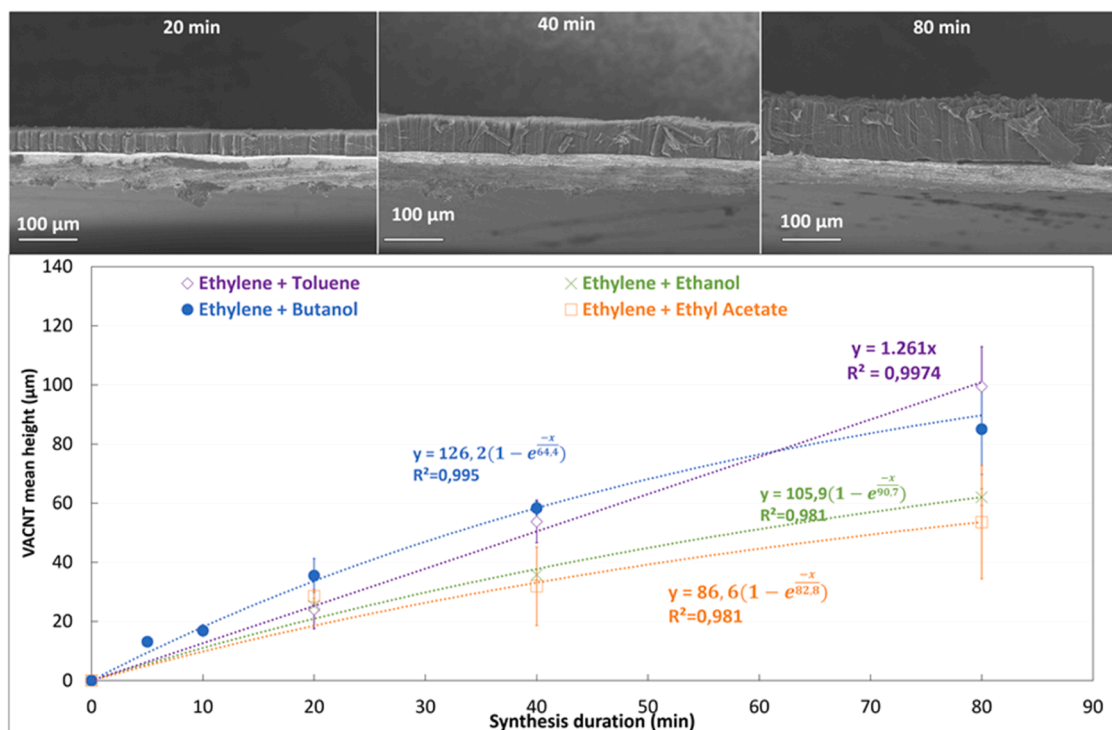


Fig. 9. Top: SEM images of VACNT height for different synthesis durations at 640 °C – (Ethylene + Butanol) Bottom: Mean VACNT height depending on precursor type and synthesis duration fitted with different models.

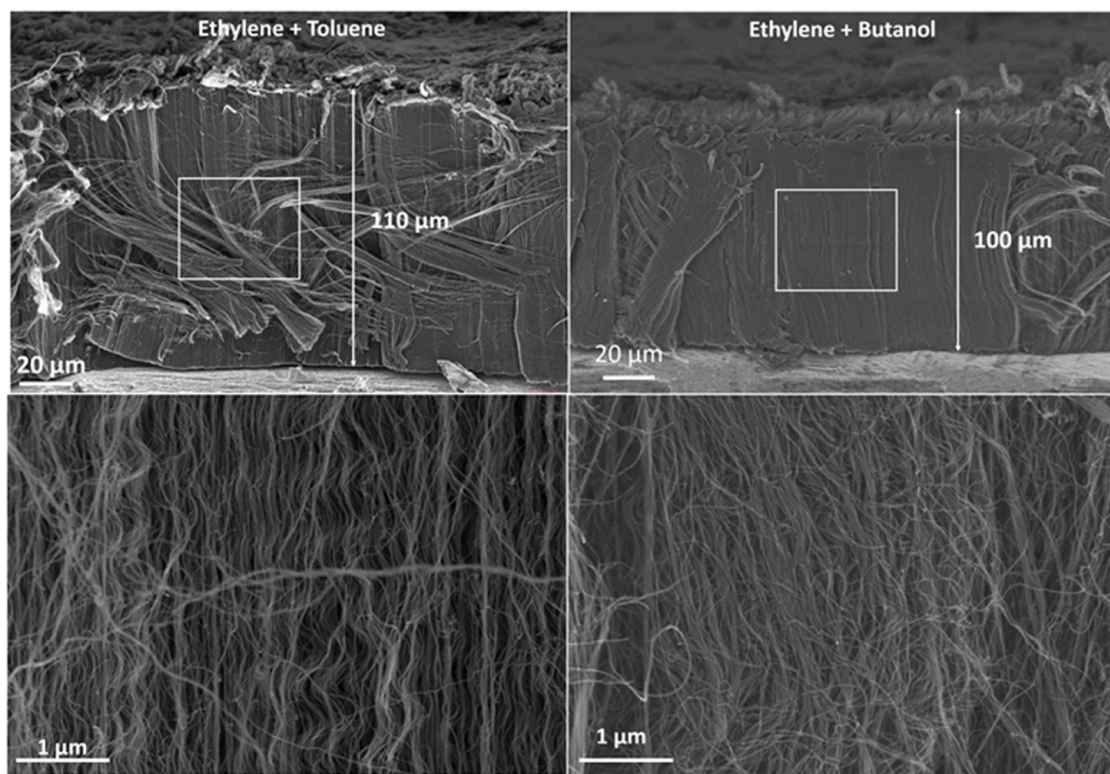


Fig. 10. SEM images of (Ethylene + Toluene) VACNT carpet (left) and (Ethylene + Butanol) VACNT carpet (right) obtained for 80 min synthesis duration from the first pellet in the reactor.

Results obtained in the present study for (ethylene + butanol) are well fitted with the exponential model (Fig. 9). Two additional syntheses at 5 min and 10 min were done to complete the study and strengthen fit accuracy. The fit gives $h_{max} = 130.2 \mu\text{m}$, $\tau = 64.4 \text{ min}$ and therefore $\gamma_0 = 1.88 \mu\text{m}\cdot\text{min}^{-1}$ for (ethylene + butanol) with a $R^2=0.997$. The maximum height value is very close to the previous results found with acetylene (121 μm [29] and 153 μm [34]) while lifetime is much higher (64 min compared to 15 min and 17 min). This could be explained by the presence of water that can increase catalyst lifetime by cleaning the catalyst particle [60] but also by the high content in hydrogen.

On the other hand, for (ethylene + toluene) results fit well with a linear model with a slope of $1.26 \mu\text{m}\cdot\text{min}^{-1}$. This means that the limitation wasn't reached after 80 min. A study needs to be carried out for (ethylene + toluene) at higher synthesis duration or with a higher ethylene concentration to confirm that no limitation is reached.

The deceleration of the growth rate with the synthesis duration could also be explained by the competition between the growth and etching of VACNTs. Indeed, the decomposition of ethanol, butanol and ethyl acetate on the catalyst produces oxidants such as water, which can etch the VACNTs [61]. This interpretation is in agreement with the differences between the O/C ratio values (Table 1). Indeed, carpets grown from precursors with the highest ratio (ethanol and ethyl acetate O/C = 1/2) are the most affected by growth rate deceleration whereas butanol with a O/C ratio of only 1/4 leads to a carpet very close in height to that of ethylene alone. Note that the VACNT sample from the pellet placed first in the reactor also reaches 100 μm in the case of the pair (ethylene + butanol) as it is the case for the (ethylene + toluene) (Fig. 10). As mentioned above for 20 min synthesis duration, if we compare the two carpets in Fig. 10, we can observe the same morphology in terms of carpet quality and cleanness. In addition, the reproducibility of this synthesis was verified (Figure S2) and proves that the process is robust, opening the way to VACNT growth at higher scale.

3.5. Additional characterizations: crystallinity, CNT diameter and density

Samples, whose synthesis conditions are reported in Table 3, are further characterized with TEM and Raman spectroscopy and are compared to the reference sample grown with acetylene from previous work [33]. As a consequence of the synthesis optimization with the new precursors, the parameters are slightly different for the bio-sourced carbon precursors compared with the reference sample: synthesis temperature is higher (640 °C vs 615 °C), synthesis duration is higher to reach almost the same VACNT height (40 min vs 20 min and 50 μm vs 65 μm) and hydrogen content is higher (50 % vs 10 %).

Raman analysis of VACNTs obtained with each precursor reveals the occurrence of the classical D, G, D3 and 2D bands (See Supplementary data). Few differences are found between precursors but the I_D/I_G ratio evolves from 1.2 to 2 when oxygen-bearing compounds are present in the reactant phase. It seems that these compounds generate defects in the CNT structure. Note that with acetylene, the ratio was found around 1.3 [29].

TEM images (Fig. 11) show clean CNTs with good structural quality with few defaults for all the precursors. No amorphous nor additional carbon are observed around carbon nanotubes. Presence of iron-based particles inside the nanotubes is observed with the same occurrence except from ethyl acetate which has a higher ferrocene content.

In addition to the VACNT height measured by SEM, the external and internal diameters were measured from TEM images (Table 3). Compared to acetylene (diameter of 8.3 nm), all the new precursors lead to a higher mean CNT external diameter: from 13.5 nm in the case of (ethylene + butanol) up to 19.2 nm in the case of (ethylene + ethyl acetate). Dörfler et al. [22] and Szabó et al. [23] reported diameter under 10 nm for ethylene on aluminum at 640 °C with a two-step CVD, to be compared with the present value of about 14 nm, but they used a mixture of Fe and Co as catalyst precursor. Lou et al. [21] obtained a diameter of 13 nm with one-step CVD at 640 °C on aluminum with ethanol, to be compared with around 16 nm here.

Table 3
Synthesis conditions and VACNT characteristics as a function of the precursor.

Precursors	Ethylene + Toluene	Ethylene + Ethanol	Ethylene + Butanol	Ethylene + Ethyl Acetate	Acetylene [33]
Synthesis Temperature (°C)	640				615
Synthesis duration (min)	40				10
Hydrogen content (%)	50				10
Ferrocene content (w %)	2.5	2	2	5	2.5
VACNT height (μm)	49	37	47	42	65
Areal mass (mg.cm ⁻²)	2.54	0.71	1.11	1.49	0.5
Density (mg.cm ⁻³)	520	193	236	359	102
Mean Internal Diameter (nm)	6.0 ± 1.6	6.9 ± 1.9	6.3 ± 1.7	8.4 ± 3.2	3.9
Mean External Diameter (nm)	13.8 ± 3.2	15.8 ± 3.7	13.5 ± 2.7	19.2 ± 6.7	8.3
Areal developed surface area (m ² .cm ⁻²)	0.412	0.094	0.191	0.174	0.141
Number of VACNT (10 ¹⁰ cm ⁻²)	20.8	6.27	9.11	5.25	11.7

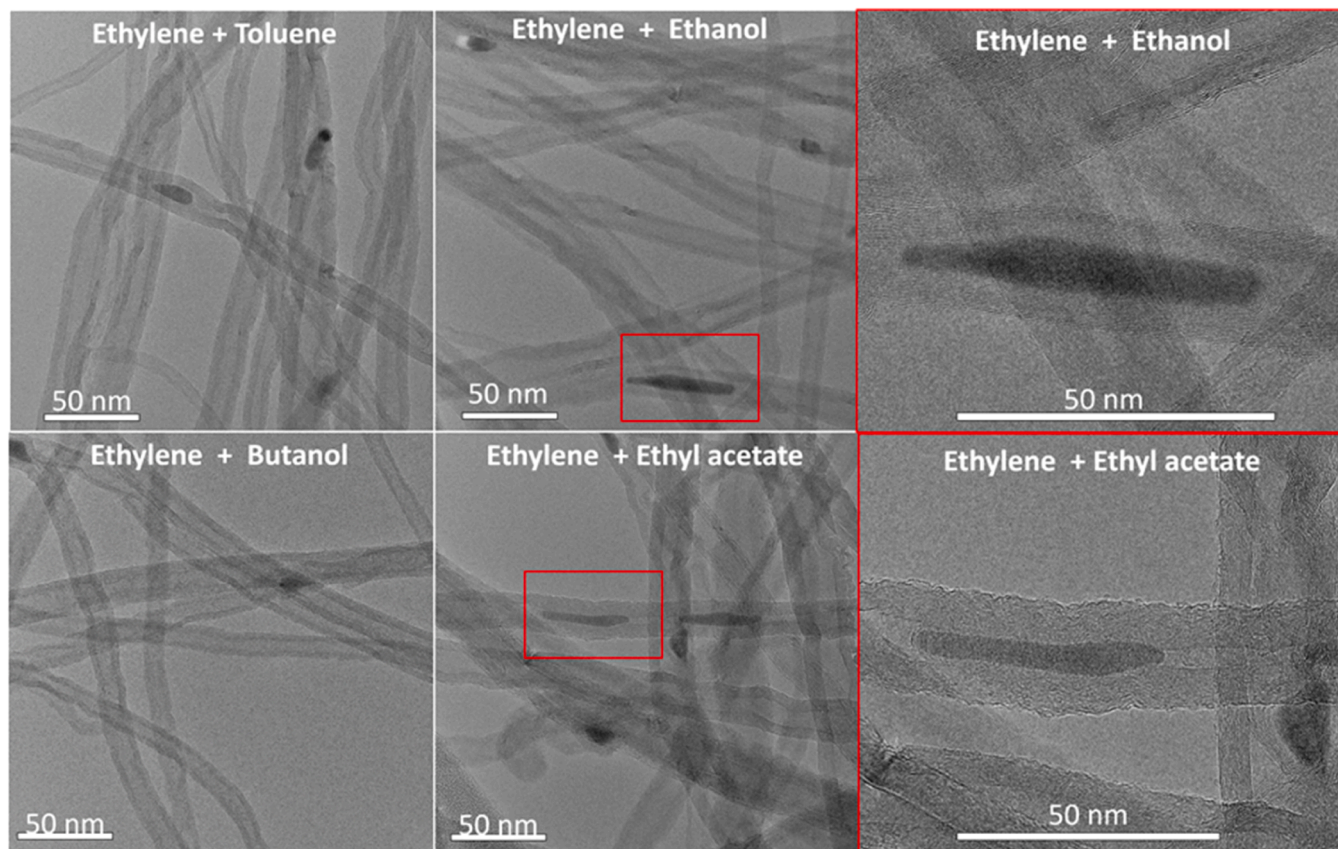


Fig. 11. TEM images for every precursors – Synthesis done at 640 °C for 40 min duration.

These CNT diameter differences between acetylene and the others precursors can be assigned to two factors. First, the syntheses were done at 640 °C with all the new precursors compared to 615 °C with acetylene. A higher temperature lead to a larger diameter [62] as we can see with (ethylene + toluene) in Fig. 12A. The VACNT diameter reaches 10.3 ± 2.7 nm at 615 °C, 11.3 ± 2.6 nm at 630 °C and 13.8 ± 3.2 nm at 640 °C. The second factor is the presence of oxidant species which affect the sintering process by improving the iron mobility on the surface induced by excess of oxygen [63]. This hypothesis is strengthened by the correlation between the number of mole of oxygen injected during the synthesis and the mean external diameter (Fig. 12B).

From these morphological data and knowing the areal mass of the different VACNT carpets, their density can be estimated, either in mass or in number of VACNT. Regarding the mass density (Table 3), all the values are greater than the one of the reference. However, (ethylene + toluene) is the more interesting couple leading to a mean value of 520 mg.cm⁻³ overpassing the 120 mg.cm⁻³ reached by Dörfler et al. [22] as

well as all the values obtained in our previous works using C₂H₂ (from 50 to 190 mg.cm³ in [11], and 80 to 350 mg.cm³ in [12]). The presence of oxygen seems to negatively influence the density since, with all the other precursors investigated in this work, the density is below 359 mg.cm⁻³, significantly lower than for (ethylene + toluene) (Table 3). This behavior must be mainly correlated with the greater values of the diameter with the oxygen-bearing precursor, which leads to a lower number density of CNT in the carpet. Indeed, the number of VACNT per cm² which reaches 2.10¹¹ CNT per cm² for (ethylene + toluene), is at least 2 times more than with other precursors. Despite the increase of the external diameter, high densities of VACNT per cm² of substrate close to and even higher than those of acetylene can be obtained.

Finally, we pay a particular attention to the determination of the areal surface area developed by each carpet (Table 3), since it corresponds to the surface of exchange involved in a lot of processes, including the electrochemical ones. The areal surface area developed by the VACNTs were inferred according to Eq. (8):

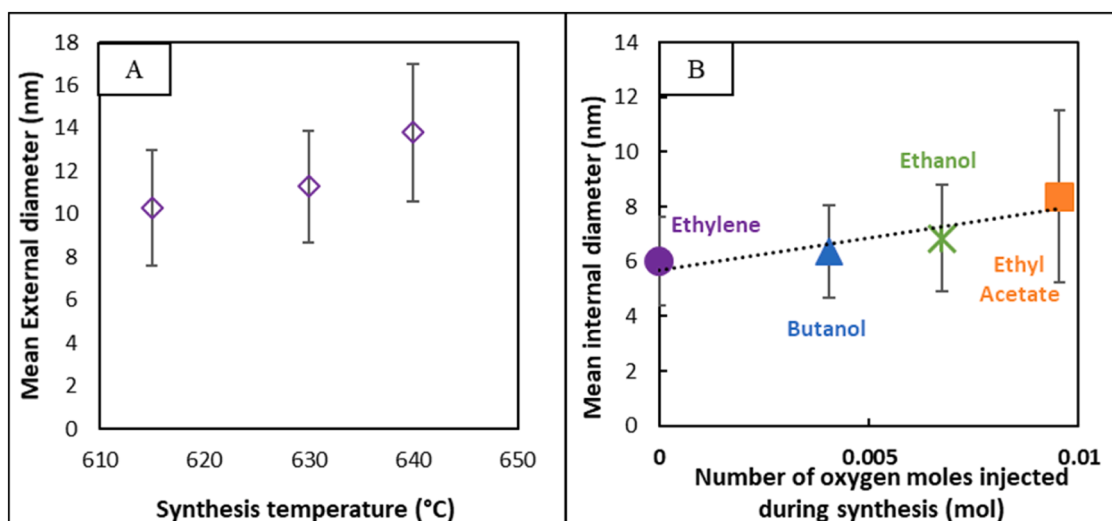


Fig. 12. A) Influence of temperature synthesis and B) carbon concentration in the feedstock on diameter of VACNT grown with (Ethylene + Toluene) during 40 min.

$$S_{developed} = \frac{m_{areal} \times D_{ext\ NT}}{\rho_{graphite} \times \left(\frac{D_{ext\ NT}^2 - D_{int\ NT}^2}{4} \right)} \quad (8)$$

Where m_{areal} is the areal mass, $D_{ext\ NT}$ is the external diameter of carbon nanotubes, $D_{int\ NT}$ is the internal diameter of carbon nanotubes, $\rho_{graphite}$ is the volumetric density of graphite.

Except the case of (ethylene + ethanol) precursors, new precursors allow to reach high developed surface area (0.174 to 0.412 $m^2.cm^{-2}$)

which are greater than the one of the reference synthesis. Furthermore, VACNTs derived from (ethylene + toluene) show the highest developed surface area with 0.412 $m^2.cm^{-2}$, which is more than twice the one of acetylene reference. These high exchange surface area are promising in terms of electrochemical applications.

3.6. Electrochemical characterization

VACNTs are specifically interesting in the fabrication of EDLC's

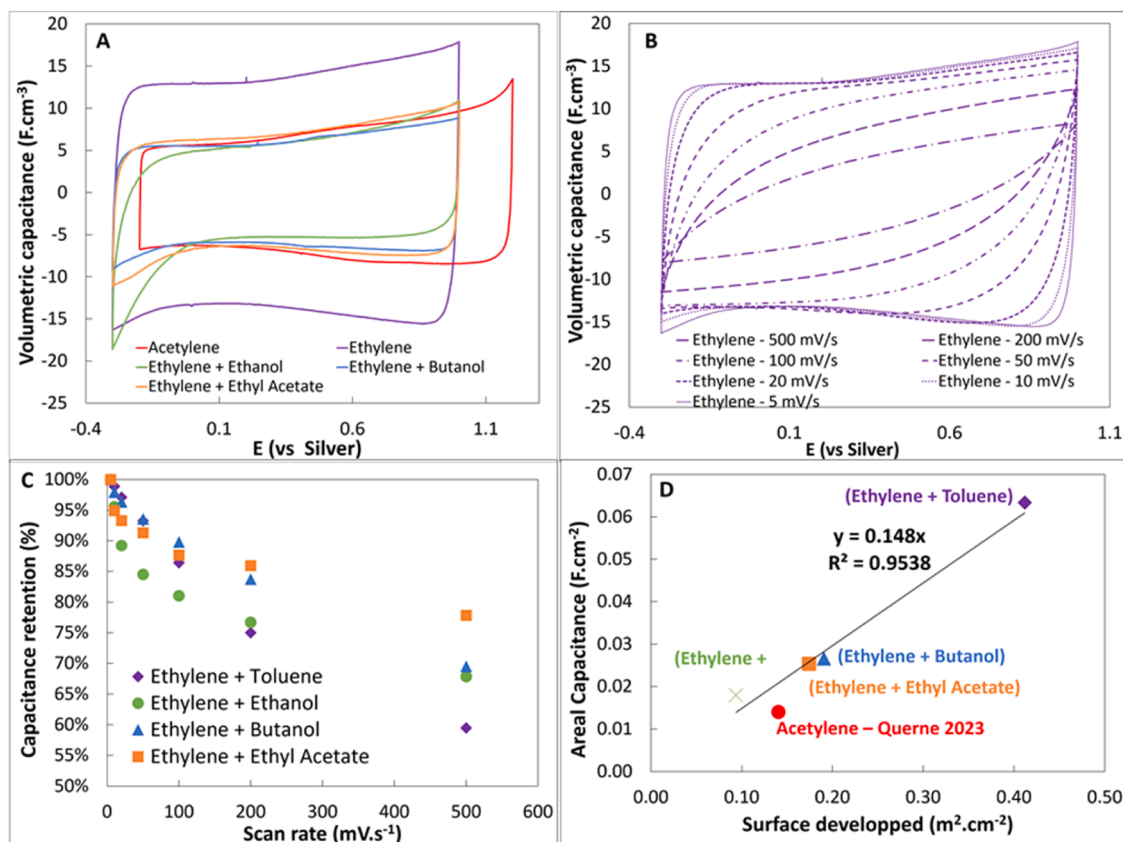


Fig. 13. (A) Specific capacitance curves of each precursor calculated from cyclic voltammograms at 5 $mV.s^{-1}$ in EMITFSI 1.3 M in ACN. (B) Volumetric capacitance of (Ethylene + Toluene) in EMITFSI 1.3 M in ACN at different scan rates. (C) Capacitance retention for every precursors tested. (D) Variation of capacitance with developed surface area and influence of the precursors on the capacitance of VACNT electrode.

electrodes [5], due to their high specific surface area and their anisotropic organization. Furthermore, they can be directly grown on electrode especially aluminum to be used as it is. Therefore, as the VACNT grown with the new precursors develop a large exchange surface area, they have been characterized as supercapacitor electrodes.

Samples of VACNT carpets grown on Al discs from each precursor are electrochemically characterized by cyclic voltammetry in EMITFSI/ACN at 1.3 M. The capacitances, C , were determined from these CV measurements (Table S1 in Supplementary data) and the volumetric capacitances, C_v , at a scan rate of $5 \text{ mV}\cdot\text{s}^{-1}$. For all the VACNT/Al electrodes, they show a quasi-rectangular shape characteristic of a capacitive behavior of carbonaceous structures (Fig. 13A). As we can see, all the precursors lead to capacitances equivalent to that of the acetylene reference, with a mean value of around $5 \text{ F}\cdot\text{cm}^{-3}$. However, with (ethylene + toluene) the VACNT carpet exhibits a higher volumetric capacitance with a mean value of $13 \text{ F}\cdot\text{cm}^{-3}$. These values are above the ones calculated from the data obtained by Dörfler et al. [22] with a C_v between $9.8 \text{ F}\cdot\text{cm}^{-3}$ and $4.8 \text{ F}\cdot\text{cm}^{-3}$.

Fig. 13B shows the specific capacitance at different scan rates for (ethylene + toluene). The shape remains quasi-rectangular up to $100 \text{ mV}\cdot\text{s}^{-1}$. At a higher scan rate the CV exhibits a more resistive behavior, mainly due to the electrolyte resistance which is high with the cell configuration used in these measurements. The volumetric capacitance decreased losing nearly 40 % (Fig. 13C). The fall is weaker for others precursors.

If we look at the variation of the capacitance as a function of the VACNT developed surface area (S_{dev}), C increases linearly with S_{dev} with a slope of $0.15 \text{ F}\cdot\text{m}^{-2}$, i.e. $15 \mu\text{F}\cdot\text{cm}^{-2}$ (Fig. 13D). This behavior and the value of the slope are close to previous work [29]. This is an indication that the VACNT carpets from the new precursors behave as VACNT carpets from acetylene when used as electrodes and that all the developed surface area is accessible to the electrolyte. As a consequence, the high volumetric capacitance obtained with (ethylene + toluene) is explained by the high surface developed by VACNT from this precursor.

Finally, this work on the development of a sustainable low-temperature one step CCVD synthesis process demonstrates that it is possible to grow VACNT exhibiting high density on aluminum from only biobased, low-toxic and eco-friendly precursors. VACNT grown from these renewable carbon sources can provide volumetric capacitance values similar or higher according to the precursor, to the one of VACNT

from acetylene from our previous work. In particular, this meets the requirements for the development of VACNT based electrodes for electrochemical storage, and raises the question of a possible industrial transfer to larger surface substrates.

3.7. Large surface synthesis

In order to demonstrate the transferability of the lab-scale process to a larger scale that meets industrial requirements for development of VACNT based materials, two syntheses with (ethylene + butanol) are achieved on large aluminum bands of 35 cm long and 5 cm wide. The reactor is a cylindrical stainless steel reactor (55 mm internal diameter) introduced in a 1 m long tubular and horizontal furnace, described elsewhere [64]. The syntheses are done at the two previously studied temperatures: 615°C and 640°C . Each synthesis lasts forty minutes.

Circular samples with a diameter of 1.2 cm were made from these two bands and observed by SEM (Fig. 14). The VACNT growth is successful at both temperatures. For the syntheses at 640°C , the carpet height is homogenous alongside the aluminum band and it was measured at $30 \pm 7 \mu\text{m}$. At 615°C no VACNT were observed on the first centimeters of the band, but after, height of $15 \mu\text{m}$ were measured.

VACNT heights are lower than the ones obtained on a smaller scale, mainly due to the differences in terms of reactor shape, gas injection system and reactor inlet geometry. Nevertheless, these results represent a step towards industrial scale-up, and further optimizations can be made to better adapt the process to large scale.

4. Conclusion

Six biobased precursors were selected to evaluate their interest to grow dense VACNTs using the one-step CCVD process: ethylene, butanol, ethyl acetate, camphor, isobutene and ethanol. After encouraging initial results under non-optimal conditions, a parametric study was carried out to optimize hydrogen content, temperature and mixing of carbon sources. VACNT carpets of up to $100 \mu\text{m}$ were obtained for (ethylene + toluene) pair and (ethylene + butanol) pair after 80 min at 640°C with good reproducibility. Precursor type influences the diameter of VACNT which increases with the presence of oxygen. Energy of activation was calculated for ethylene, butanol and (ethylene + butanol) highlighting two different limiting step depending on the precursor.

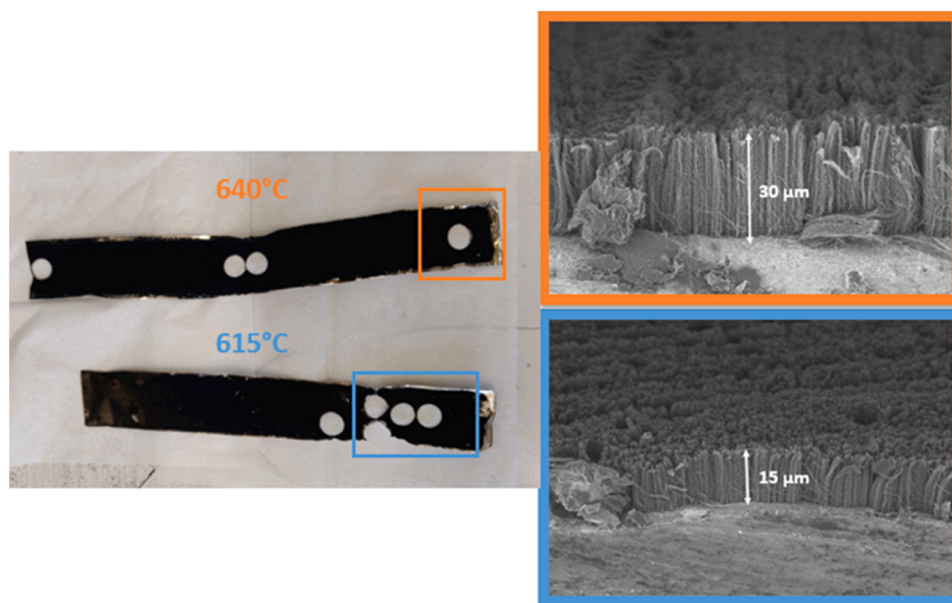


Fig. 14. Left: Photo of the two aluminum bands after synthesis at the two different temperatures. Right: SEM images of the carpet obtained on the aluminum band at 615°C and 640°C .

Electrochemical characterization shows that the (ethylene + toluene) pair exhibits a higher volumetric capacitance than our reference with acetylene. However, the volumetric capacitances of samples derived from oxygen-containing precursors are lower due to lower carpet density, but are nearly equivalent to the one of the reference with acetylene. Syntheses with the (ethylene + butanol) pair were scaled-up on larger aluminum samples paving the way to its development at the industrial level. This work proves that dense VACNTs can be obtained with biobased carbon sources and low-toxicity precursors on aluminum thereby reducing the carbon footprint of the VACNT CVD process. Other applications can be targeted to further highlight the advantage of using biobased precursors.

CRedit authorship contribution statement

Corentin Chatelet: Writing – original draft, Investigation, Formal analysis, Conceptualization. **Ugo Forestier-Colleoni:** Investigation. **Philippe Banet:** Writing – review & editing, Supervision, Formal analysis, Data curation, Conceptualization. **Jérémy Descarpentries:** Writing – review & editing, Supervision, Formal analysis. **Thomas Goislard de Monsabert:** Writing – review & editing, Supervision, Formal analysis. **Fabien Nassoy:** Investigation. **Cécile Reynaud:** Writing – review & editing, Writing – original draft, Methodology, Data curation. **Mathieu Pinault:** Writing – review & editing, Writing – original draft, Supervision, Project administration, Funding acquisition, Formal analysis, Conceptualization.

Declaration of competing interest

The authors declare the following financial interests/personal relationships which may be considered as potential competing interests: Corentin Chatelet reports financial support was provided by NAWAH (ANRT/CIFRE N°2021/0185). Corentin Chatelet reports a relationship with NawaH that includes: employment. If there are other authors, they declare that they have no known competing financial interests or personal relationships that could have appeared to influence the work reported in this paper.

Acknowledgement

The authors would like to thanks E.Larquet (CIMEX) for access to TEM, E.Charon (CEA-Saclay) for Raman analysis, V.Mertens (CEA-Saclay) for the support on the SEM observations and D.Porterat for the maintenance of the synthesis equipment.

Supplementary materials

Supplementary material associated with this article can be found, in the online version, at [doi:10.1016/j.cartre.2024.100450](https://doi.org/10.1016/j.cartre.2024.100450).

Data availability

The data that has been used is confidential.

References

- IEA (2020), Global energy-related CO₂ emissions by sector, IEA, Paris <https://www.iea.org/data-and-statistics/charts/global-energy-related-co2-emissions-by-sector>, Licence: CC BY 4.0, n.d.
- M.M. Titirici, R.J. White, N. Brun, V.L. Budarin, D.S. Su, F. Del Monte, J.H. Clark, M.J. MacLachlan, Sustainable carbon materials, *Chem. Soc. Rev.* 44 (2015) 250–290, <https://doi.org/10.1039/C4CS00232F>.
- W. Shi, D.L. Plata, Vertically aligned carbon nanotubes: production and applications for environmental sustainability, *Green Chem* 20 (2018) 5245–5260, <https://doi.org/10.1039/C8GC02195C>.
- Yuanyuan Li, Fu-Gang Zhao, Li-Na Liu, Zi-Wen Xu, Guanghui Xie, Jingjing Li, Tianzeng Gao, Wenguo Li, Wei-Shi Li, Carbon Nanomaterials-enabled High-performance supercapacitors : a Review, *Adv. Energy Sustain. Resour* (2023), <https://doi.org/10.1002/aesr.202200152>.
- H. Zhang, G. Cao, Y. Yang, Z. Gu, Comparison between electrochemical properties of aligned carbon nanotube array and entangled carbon nanotube electrodes, *J. Electrochem. Soc.* 155 (2008) K19, <https://doi.org/10.1149/1.2811864>.
- V. Jourdain, C. Bichara, Current understanding of the growth of carbon nanotubes in catalytic chemical vapour deposition, *Carbon N Y* 58 (2013) 2–39, <https://doi.org/10.1016/j.carbon.2013.02.046>.
- T.A. Ewing, N. Nouse, M. Van Lint, J. Van Haveren, J. Hugenholtz, D.S. Van Es, Fermentation for the production of biobased chemicals in a circular economy: a perspective for the period 2022–2050, *Green Chem* 24 (2022) 6373–6405, <https://doi.org/10.1039/D1GC04758B>.
- Y. Zhou, J. He, R. Chen, X. Li, Recent advances in biomass-derived graphene and carbon nanotubes, *Mater. Today Sustain.* 18 (2022) 100138, <https://doi.org/10.1016/j.mtsust.2022.100138>.
- A.B. Suriani, R. Md Nor, M. Rusop, Vertically aligned carbon nanotubes synthesized from waste cooking palm oil, *J. Ceram. Soc. Jpn.* 118 (2010) 963–968, <https://doi.org/10.2109/jcersj2.118.963>.
- A.B. Suriani, A.A. Azira, S.F. Nik, R. Md Nor, M. Rusop, Synthesis of vertically aligned carbon nanotubes using natural palm oil as carbon precursor, *Mater. Lett.* 63 (2009) 2704–2706, <https://doi.org/10.1016/j.matlet.2009.09.048>.
- P. Ghosh, R.A. Afre, T. Soga, T. Jimbo, A simple method of producing single-walled carbon nanotubes from a natural precursor: eucalyptus oil, *Mater. Lett.* 61 (2007) 3768–3770, <https://doi.org/10.1016/j.matlet.2006.12.030>.
- R.A. Afre, T. Soga, T. Jimbo, M. Kumar, Y. Ando, M. Sharon, Growth of vertically aligned carbon nanotubes on silicon and quartz substrate by spray pyrolysis of a natural precursor: turpentine oil, *Chem. Phys. Lett.* 414 (2005) 6–10, <https://doi.org/10.1016/j.cplett.2005.08.040>.
- R. Kumar, R.S. Tiwari, O.N. Srivastava, Scalable synthesis of aligned carbon nanotubes bundles using green natural precursor: neem oil, *Nanoscale Res. Lett.* 6 (2011) 92, <https://doi.org/10.1186/1556-276X-6-92>.
- A. Termehyousefi, S. Bagheri, K. Shinji, J. Rouhi, M. Rusop Mahmood, S. Ikeda, Fast synthesis of multilayer carbon nanotubes from camphor oil as an energy storage material, *BioMed Res. Int.* 2014 (2014) 1–6, <https://doi.org/10.1155/2014/691537>.
- M. Pavese, S. Musso, S. Bianco, M. Giorelli, N. Pugno, An analysis of carbon nanotube structure wettability before and after oxidation treatment, *J. Phys. Condens. Matter* 20 (2008) 474206, <https://doi.org/10.1088/0953-8984/20/47/474206>.
- S. Musso, G. Fanchini, A. Tagliaferro, Growth of vertically aligned carbon nanotubes by CVD by evaporation of carbon precursors, *Diam. Relat. Mater.* 14 (2005) 784–789, <https://doi.org/10.1016/j.diamond.2004.12.030>.
- M. Ahmad, S.R.P. Silva, Low temperature growth of carbon nanotubes – A review, *Carbon N Y* 158 (2020) 24–44, <https://doi.org/10.1016/j.carbon.2019.11.061>.
- P. Jiang, G. Zhao, H. Zhang, T. Ji, L. Mu, X. Lu, J. Zhu, Towards carbon neutrality of calcium carbide-based acetylene production with sustainable biomass resources, *Green Energy Environ* (2022) S2468025722001820, <https://doi.org/10.1016/j.gee.2022.12.004>.
- M. Ballesteros, P. Manzanares, Liquid Biofuels, Role bioenergy bioeconomy, *Elsevier* (2019) 113–144, <https://doi.org/10.1016/B978-0-12-813056-8.00003-0>.
- N. Yoshikawa, T. Asari, N. Kishi, S. Hayashi, T. Sugai, H. Shinohara, An efficient fabrication of vertically aligned carbon nanotubes on flexible aluminum foils by catalyst-supported chemical vapor deposition, *Nanotechnology* 19 (2008) 245607, <https://doi.org/10.1088/0957-4484/19/24/245607>.
- F. Lou, H. Zhou, F. Huang, F. Vullum-Bruer, T.D. Tran, D. Chen, Facile synthesis of manganese oxide/aligned carbon nanotubes over aluminum foil as 3D binder free cathodes for lithium ion batteries, *J. Mater. Chem. A* 1 (2013) 3757, <https://doi.org/10.1039/c3ta00793f>.
- S. Dörfler, I. Felhösi, T. Marek, S. Thieme, H. Althues, L. Nyikos, S. Kaskel, High power supercap electrodes based on vertical aligned carbon nanotubes on aluminum, *J. Power Sources* 227 (2013) 218–228, <https://doi.org/10.1016/j.jpowsour.2012.11.068>.
- A. Szabó, E. Kecsenovity, Z. Pápa, T. Gyulavári, K. Németh, E. Horvath, K. Hernadi, Influence of synthesis parameters on CCVD growth of vertically aligned carbon nanotubes over aluminum substrate, *Sci. Rep.* 7 (2017) 9557, <https://doi.org/10.1038/s41598-017-10055-0>.
- T. Yan, M. Zhang, R. Yuan, W. Dai, Catalytic upgrading biomass-derived ethanol and acetic acid into C₄ chemicals, *Sci. China Chem.* 67 (2024) 3588–3613, <https://doi.org/10.1007/s11426-024-2250-9>.
- A. Shibuya, G. Chen, A. Miyoshi, D.N. Futaba, Improving the synthetic efficiency of single-wall carbon nanotube forests using a gas-analysis-designed mixed carbon feedstock, *Carbon N Y* 170 (2020) 59–65, <https://doi.org/10.1016/j.carbon.2020.08.001>.
- D.L. Plata, E.R. Meshot, C.M. Reddy, A.J. Hart, P.M. Gschwend, Multiple alkynes react with ethylene to enhance carbon nanotube synthesis, suggesting a polymerization-like formation mechanism, *ACS Nano* 4 (2010) 7185–7192, <https://doi.org/10.1021/nn101842g>.
- M. Pinault, V. Pichot, H. Khodja, P. Launois, C. Reynaud, M. Mayne-L'Hermite, Evidence of sequential lift in growth of aligned multiwalled carbon nanotube multilayers, *Nano Lett* 5 (2005) 2394–2398, <https://doi.org/10.1021/nl051472k>.
- E. Charon, M. Pinault, M. Mayne-L'Hermite, C. Reynaud, One-step synthesis of highly pure and well-crystallized vertically aligned carbon nanotubes, *Carbon N Y* 173 (2021) 758–768, <https://doi.org/10.1016/j.carbon.2020.10.056>.
- F. Nassoy, M. Pinault, J. Descarpentries, T. Vignal, P. Banet, P.E. Coulon, T. Goislard de Monsabert, H. Hauf, P.H. Aubert, C. Reynaud, M. Mayne-L'Hermite, Single-step synthesis of vertically aligned carbon nanotube forest on Aluminium foils, *Nanomaterials* 9 (2019) 1590, <https://doi.org/10.3390/nano9111590>.

- [30] M.R. Arcila-Velez, J. Zhu, A. Childress, M. Karakaya, R. Podila, A.M. Rao, M. E. Roberts, Roll-to-roll synthesis of vertically aligned carbon nanotube electrodes for electrical double layer capacitors, *Nano Energy* 8 (2014) 9–16, <https://doi.org/10.1016/j.nanoen.2014.05.004>.
- [31] P. Boulanger, L. Belkadi, J. Descarpentries, D. Porterat, E. Hibert, A. Brouzes, M. Mille, S. Patel, M. Pinault, C. Reynaud, M. Mayne-L'Hermite, J.M. Decamps, Towards large scale aligned carbon nanotube composites: an industrial safe-by-design and sustainable approach, *J. Phys. Conf. Ser.* 429 (2013) 012050, <https://doi.org/10.1088/1742-6596/429/1/012050>.
- [32] S.S. Meysami, A.A. Koós, F. Dillon, M. Dutta, N. Grobert, Aerosol-assisted chemical vapour deposition synthesis of multi-wall carbon nanotubes: III. Towards upscaling, *Carbon N Y* 88 (2015) 148–156, <https://doi.org/10.1016/j.carbon.2015.02.045>.
- [33] C. Querne, T. Vignal, M. Pinault, P. Banet, M. Mayne-L'Hermite, P.H. Aubert, A comparative study of high density Vertically Aligned Carbon Nanotubes grown onto different grades of aluminum – Application to supercapacitors, *J. Power Sources* 553 (2023) 232258, <https://doi.org/10.1016/j.jpowsour.2022.232258>.
- [34] A. Combrisson, E. Charon, M. Pinault, C. Reynaud, M. Mayne-L'Hermite, Critical role of the acetylene content and Fe/C ratio on the thickness and density of vertically aligned carbon nanotubes grown at low temperature by a one-step catalytic chemical vapor deposition process, *Nanomaterials* 12 (2022) 2338, <https://doi.org/10.3390/nano12142338>.
- [35] M. Chase, NIST-JANAF thermochemical tables, 4th Edition, American Institute of Physics, 1, 1998.
- [36] D.A. Pittam, G. Pilcher, Measurements of heats of combustion by flame calorimetry. Part 8.—Methane, ethane, propane, n-butane and 2-methylpropane, *J. Chem. Soc. Faraday Trans. 1 Phys. Chem. Condens. Phases* 68 (1972) 2224, <https://doi.org/10.1039/f19726802224>.
- [37] W.V. Steele, The standard enthalpies of formation of bicyclic compounds III. 1,7,7-trimethylbicyclo[2.2.1]heptan-2-one, *J. Chem. Thermodyn.* 9 (1977) 311–314, [https://doi.org/10.1016/0021-9614\(77\)90051-9](https://doi.org/10.1016/0021-9614(77)90051-9).
- [38] C. Mosselmaann, D. Harmdekker, Enthalpies of Formation of n-Alkan-1-01s, (n.d.).
- [39] J. Chao, F.D. Rossini, Heats of Combustion, Formation, and Isomerization of Nineteen Alkanols, *J. Chem. Eng. Data* 10 (1965) 374–379, <https://doi.org/10.1021/je60027a022>.
- [40] K.B. Wiberg, L.S. Crocker, K.M. Morgan, Thermochemical studies of carbonyl compounds. 5. Enthalpies of reduction of carbonyl groups, *J. Am. Chem. Soc.* 113 (1991) 3447–3450, <https://doi.org/10.1021/ja00009a033>.
- [41] C. Castro, M. Pinault, S. Coste-Leconte, D. Porterat, N. Bendiab, C. Reynaud, M. Mayne-L'Hermite, Dynamics of catalyst particle formation and multi-walled carbon nanotube growth in aerosol-assisted catalytic chemical vapor deposition, *Carbon N Y* 48 (2010) 3807–3816, <https://doi.org/10.1016/j.carbon.2010.06.045>.
- [42] C. Castro, M. Pinault, D. Porterat, C. Reynaud, M. Mayne-L'Hermite, The role of hydrogen in the aerosol-assisted chemical vapor deposition process in producing thin and densely packed vertically aligned carbon nanotubes, *Carbon N Y* 61 (2013) 585–594, <https://doi.org/10.1016/j.carbon.2013.05.040>.
- [43] M.S. Mamat, G.S. Walker, D.M. Grant, Y. Yaakob, N.A. Shaharun, Effect of the reaction temperature and ethene/hydrogen composition on the nanostructured carbon produced by CVD using supported NiFe₂O₄ as a catalyst, *Results Phys* 19 (2020) 103497, <https://doi.org/10.1016/j.rinp.2020.103497>.
- [44] M.J. Behr, E.A. Gaulding, K.A. Mkhoyan, E.S. Aydil, Effect of hydrogen on catalyst nanoparticles in carbon nanotube growth, *J. Appl. Phys.* 108 (2010) 053303, <https://doi.org/10.1063/1.3467971>.
- [45] C. Zhuo, H. Richter, Y.A. Levendis, Carbon nanotube production from ethylene in CO₂/N₂ environments, *J. Energy Resour. Technol.* 140 (2018) 085001, <https://doi.org/10.1115/1.4039328>.
- [46] M. Rosi, D. Skouteris, N. Balucani, C. Nappi, N. Faginas Lago, L. Pacifici, S. Falcinelli, D. Stranges, An Experimental and Theoretical Investigation of 1-Butanol Pyrolysis, *Front. Chem.* 7 (2019) 326, <https://doi.org/10.3389/fchem.2019.00326>.
- [47] D.C. Vargas, S. Salazar, J.R. Mora, K.M. Van Geem, D.Almeida Streitwieser, Experimental and theoretical study of the thermal decomposition of ethyl acetate during fast pyrolysis, *Chem. Eng. Res. Des.* 157 (2020) 153–161, <https://doi.org/10.1016/j.cherd.2020.03.001>.
- [48] A.V. Minakov, M.M. Simunin, I.I. Ryzhkov, Modelling of ethanol pyrolysis in a commercial CVD reactor for growing carbon layers on alumina substrates, *Int. J. Heat Mass Transf.* 145 (2019) 118764, <https://doi.org/10.1016/j.ijheatmasstransfer.2019.118764>.
- [49] C. Singh, M.S.P. Shaffer, A.H. Windle, Production of controlled architectures of aligned carbon nanotubes by an injection chemical vapour deposition method, *Carbon N Y* 41 (2003) 359–368, [https://doi.org/10.1016/S0008-6223\(02\)00314-7](https://doi.org/10.1016/S0008-6223(02)00314-7).
- [50] C.T. Wirth, C. Zhang, G. Zhong, S. Hofmann, J. Robertson, Diffusion- and reaction-limited growth of carbon nanotube forests, *ACS Nano* 3 (2009) 3560–3566, <https://doi.org/10.1021/nm900613e>.
- [51] W.H. Chiang, R.M. Sankaran, Microplasma synthesis of metal nanoparticles for gas-phase studies of catalyzed carbon nanotube growth, *Appl. Phys. Lett.* 91 (2007) 121503, <https://doi.org/10.1063/1.2786835>.
- [52] W.H. Chiang, R.M. Sankaran, Relating carbon nanotube growth parameters to the size and composition of nanocatalysts, *Diam. Relat. Mater.* 18 (2009) 946–952, <https://doi.org/10.1016/j.diamond.2009.01.010>.
- [53] M.V. Kharlamova, Investigation of growth dynamics of carbon nanotubes, *Beilstein J. Nanotechnol.* 8 (2017) 826–856, <https://doi.org/10.3762/bjnano.8.85>.
- [54] G. Chen, R.C. Davis, H. Kimura, S. Sakurai, M. Yumura, D.N. Futaba, K. Hata, The relationship between the growth rate and the lifetime in carbon nanotube synthesis, *Nanoscale* 7 (2015) 8873–8878, <https://doi.org/10.1039/C5NR01125F>.
- [55] B. McLean, I. Mitchell, F. Ding, Mechanism of alcohol chemical vapor deposition growth of carbon nanotubes: catalyst oxidation, *Carbon N Y* 191 (2022) 1–9, <https://doi.org/10.1016/j.carbon.2022.01.046>.
- [56] R. Xiang, Z. Yang, Q. Zhang, G. Luo, W. Qian, F. Wei, M. Kadowaki, E. Einarsson, S. Maruyama, Growth deceleration of vertically aligned carbon nanotube arrays: catalyst deactivation or feedstock diffusion controlled? *J. Phys. Chem. C* 112 (2008) 4892–4896, <https://doi.org/10.1021/jp710730x>.
- [57] E. Einarsson, Y. Murakami, M. Kadowaki, S. Maruyama, Growth dynamics of vertically aligned single-walled carbon nanotubes from in situ measurements, *Carbon N Y* 46 (2008) 923–930, <https://doi.org/10.1016/j.carbon.2008.02.021>.
- [58] H. Almkhelfe, J. Carpena-Núñez, T.C. Back, P.B. Amama, Gaseous product mixture from Fischer-Tropsch synthesis as an efficient carbon feedstock for low temperature CVD growth of carbon nanotube carpets, (n.d.) 31.
- [59] A.A. Puzetzk, D.B. Geoghegan, S. Jesse, I.N. Ivanov, G. Eres, In situ measurements and modeling of carbon nanotube array growth kinetics during chemical vapor deposition, *Appl. Phys. A* 81 (2005) 223–240, <https://doi.org/10.1007/s00339-005-3256-7>.
- [60] P.B. Amama, C.L. Pint, L. McJilton, S.M. Kim, E.A. Stach, P.T. Murray, R.H. Hauge, B. Maruyama, Role of water in super growth of single-walled carbon nanotube carpets, *Nano Lett* 9 (2009) 44–49, <https://doi.org/10.1021/nl801876h>.
- [61] X. Zheng, Z. Zhang, G. Zhou, M. Zou, F. Zhang, P.X. Hou, C. Shi, H.M. Cheng, M. Wang, C. Liu, Efficient fabrication of single-wall carbon nanotube nanoreactors by defect-induced cutting, *Nanoscale* 15 (2023) 3931–3939, <https://doi.org/10.1039/D2NR06696C>.
- [62] M. Picher, E. Anglaret, R. Arenal, V. Jourdain, Processes controlling the diameter distribution of single-walled carbon nanotubes during catalytic chemical vapor deposition, *ACS Nano* 5 (2011) 2118–2125, <https://doi.org/10.1021/nn1033086>.
- [63] W. Shi, J. Li, E.S. Polsen, C.R. Oliver, Y. Zhao, E.R. Meshot, M. Barclay, D. H. Fairbrother, A.J. Hart, D.L. Plata, Oxygen-promoted catalyst sintering influences number density, alignment, and wall number of vertically aligned carbon nanotubes, *Nanoscale* 9 (2017) 5222–5233, <https://doi.org/10.1039/C6NR09802A>.
- [64] S. Patel, Y. Magga, L. Belkady, E. Hibert, D. Porterat, P. Boulanger, M. Pinault, M. Mayne-L'Hermite, Development and optimization of a secure injection CVD process to grow aligned carbon nanotubes on large substrates, *J. Phys. Conf. Ser.* 429 (2013) 012053, <https://doi.org/10.1088/1742-6596/429/1/012053>.